



MOLECULAR DYNAMICS STUDY OF THE STRUCTURE AND PROPERTIES OF TWIST BOUNDARIES

C. Counterman, L.-Q. Chen, G. Kalonji

► To cite this version:

C. Counterman, L.-Q. Chen, G. Kalonji. MOLECULAR DYNAMICS STUDY OF THE STRUCTURE AND PROPERTIES OF TWIST BOUNDARIES. *Journal de Physique Colloques*, 1988, 49 (C5), pp.C5-139-C5-150. 10.1051/jphyscol:1988511 . jpa-00228008

HAL Id: jpa-00228008

<https://hal.science/jpa-00228008>

Submitted on 4 Feb 2008

HAL is a multi-disciplinary open access archive for the deposit and dissemination of scientific research documents, whether they are published or not. The documents may come from teaching and research institutions in France or abroad, or from public or private research centers.

L'archive ouverte pluridisciplinaire **HAL**, est destinée au dépôt et à la diffusion de documents scientifiques de niveau recherche, publiés ou non, émanant des établissements d'enseignement et de recherche français ou étrangers, des laboratoires publics ou privés.

MOLECULAR DYNAMICS STUDY OF THE STRUCTURE AND PROPERTIES OF TWIST BOUNDARIES

C. COUNTERMAN, L.-Q. CHEN and G. KALONJI

*Department of Materials Science and Engineering, Massachusetts
Institute of Technology, Cambridge, MA 02139, U.S.A.*

Abstract - Molecular dynamics simulations of the structure and thermodynamic properties of $\Sigma 5$ (001) twist boundaries were performed. The systems interacted through interatomic potential functions chosen to represent Ar and NaCl, and the simulations were conducted over a range of temperatures from low temperature to bulk melting. Excess thermodynamic properties were calculated through the use of perfect crystal reference systems. Structural changes with temperature were assessed with a variety of techniques, including the use of bicrystal Patterson functions. Both systems exhibit significant disordering at the grain boundaries at temperatures below bulk melting, a disorder which increases quite continuously with temperature. The NaCl system remains well ordered up to much higher relative temperatures than does the Ar system.

INTRODUCTION

Detailed information concerning the local atomic structure of grain boundaries has been the goal of innumerable experimental and theoretical studies in recent years. The logical starting point which has been employed by many groups is to attempt to understand the structure of the simple, short coincidence period boundaries first. In fact, those performing atomistic computer simulation studies have, in the past, had little choice in this matter given the computational resources required to do much else. Among the simple, short period boundaries which have received the most attention in both simulation and experiment is the $\Sigma 5$ (001) twist boundary in fcc metals. There have been a number of experimental studies and some atomistic simulation work and little agreement found between the two.

In an attempt to elucidate relationships between boundary structure and properties with temperature in twists boundaries we undertook a molecular dynamics (MD) study of $\Sigma 5$ (001) boundaries in two different systems. In the first system the particles interacted through the Lennard-Jones potential with parameters chosen to represent argon. The second simulation was of a $\Sigma 5$ (001) twist boundary in NaCl. The goal of our research was to study the structure and properties of these

model bicrystals over a wide range of temperatures, from low temperature to bulk melting. We calculated the excess thermodynamic properties of the grain boundaries through the use of perfect crystal reference systems, using methods we have employed and described elsewhere /1/. One of our interests was to assess the concept of structural multiplicity in twist boundaries which had been proposed on the basis of molecular statics studies /2/, and observed in limited molecular dynamics runs /3/. We were also interested in determining whether twists boundaries undergo phase transitions at higher temperatures similar to those we had earlier observed in tilt boundaries using MD simulation /4,5/.

There has been a fair amount of study both theoretically and experimentally on grain boundaries in ionic materials. A number of experimental studies indicate the stability of twist boundaries in ionic materials /6,7/. In contrast recent computer simulations of structure and energy of (001) twist boundaries in alkali halides /8/ and MgO /9/ employing molecular statics techniques showed no cusps near special misorientations in (001) twist boundaries. Moreover, these calculations suggest that without creating point defects (001) twist boundaries should be only marginally stable with respect to the breakup of the bicrystal into two free surfaces. An inspection of the grain boundary structure showed that not only does coincidence occur where ions of opposite charges face one another across the grain boundary, but anti-coincidences, where like ion pairs are present at the boundary, are also present. Introduction of Fe^{2+} into the (001) twist boundary in MgO increases the stability of the simulated boundary but not enough for it to be stable at finite temperatures /10/. On the other hand a very stable structure was found for a $\Sigma 5$ twist boundary in NiO by introducing a pair of Shottky defects per CSL unit cell /11/. Our study of $\Sigma 5$ twist boundaries in NaCl had two goals. First we wanted to find out whether or not the stable configuration generated by Tasker and Duffy /11/ is also stable under dynamical conditions. Our second goal was to determine whether or not grain boundaries in ionic materials undergo any structural transitions, such as grain boundary melting or disordering.

For the simulations of both the Ar and the NaCl bicrystals we employed the flexible borders formulation of molecular dynamics /12/. It is unwise to attempt to study structural phase transitions in solids with conventional microcanonical MD simulations as the constant volume constraint precludes changes in computational cell size and shape. Our simulations of NaCl boundaries were performed in the isenthalpic-isostress ensemble. For the simulations of Ar bicrystals we rescaled atomic velocities to maintain constant temperature. All of the systems were simulated under hydrostatic pressure.

To examine details of the structure, and particularly to examine correlations at higher temperatures, we used Harker-Patterson sections through the Patterson function of the system /13/. In our research we often find it useful to employ a defect location algorithm, which consists of counting the number of atoms within a given radius, in order to limit the atoms contributing to the Patterson function to those which are part of the grain boundary.

SIMULATIONS OF THE LENNARD-JONES $\Sigma 5$ TWIST BOUNDARY

We simulated a $\Sigma 5$ (001) twist boundary in an argon system which contained 5000 atoms. The simulation cell contained 25 units of the CSL building block, five on a side, and had 20 atomic layers in each crystal of the bicrystal. We enforced periodic boundary conditions in all directions, so the system contained two $\Sigma 5$ twist boundaries. The cut-off range was chosen to fall between third and fourth nearest neighbors, and was scaled with temperature.

Low T relaxed structure: Our first task was to determine the low temperature relaxed structure. Our initial configuration consisted of two fcc crystals with a 36.87° misorientation, to produce a $\Sigma 5$ (001) boundary, with no expansion at the boundary or relative translation in the grain boundary plane. This system was relaxed to equilibrium at low temperature under constant hydrostatic pressure. Local and global relaxations were allowed. The relaxed structure is illustrated in Figure 1. An important feature of the structure is the volume relaxation at the grain boundary

plane. We see an expansion normal to the boundary plane of $\sim 20\%$ of an interplanar spacing. The planes in the relaxed average structure were distorted symmetrically about each interface. The significant local relaxations at the grain boundary plane involve motion of the coincident atoms towards the boundary by $\sim .104$ (where the interatomic distance is ~ 1.1) units with respect to the rest of the atoms in that plane. This aspect of the structure can be seen in Figure 2. The thickness of a plane as measured by the statistical variance of the coordinates of the atoms with respect to the average for that plane decreases from $.001733$ in the plane adjacent to the interface, to $.00005476$ in the second, to 0.00000001 in the fifth.

In order to determine whether there are other stable translational states than the CSL configuration described above we performed a series of MD simulations using the so-called Type 1 and Type 2 translations of Bristowe and Crocker /14/ which they found to be metastable in statics calculations. However both of these translation states were found to be unstable in our constant pressure MD simulations, though we confirmed that the Type 2 is metastable under constant volume conditions. We therefore settled on the CSL translation state and this relaxed structure was used as the starting structure for the temperature variation experiments.

Changes in Structure with Temperature

The experimental conditions were largely the same as described in /1/. A constant hydrostatic pressure of $.1$ reduced units was applied. The duration of experiments was 6000 time steps, with averages taken after time step 2000. The starting atomic arrangements were the relaxed low temperature configuration, with positions scaled to reach the expected equilibrium interatomic spacings for the experimental temperature, which sped the approach to equilibrium.

The first qualitative changes in the structure begin to appear at a temperature of $.055$ reduced units, corresponding to $\sim 1/3 T_m$. As can be seen in Figure 3, a portion on the boundary has exhibited what we call a pop-through, which is a region where 4 atoms in a plane adjacent to the boundary have fallen into the boundary and rotated into the orientation of the other crystal, thereby joining the other crystal and in effect moving the interface by one atomic layer. These pop-throughs are a part of the dynamical structure of the boundary, though they do involve an increase, though minor, in boundary enthalpy. This pop-through survives and is joined by another at $T = .090$. As the temperature is raised further, they become increasingly common, and may occur in adjacent units. At temperatures above $.08$, a noticeable relative translation of the crystals occurs. This translation is less than $1/2$ the Type 1 or Type 2 translations. It is not a function of temperature (and in fact is not present in the simulation at $.150$), and is not stable at low temperatures. The pop-throughs are detectable to $T = .135$. At higher temperatures the structure is disordered enough to make identification difficult. In fact, given the large magnitude of atomic fluctuations in the boundary at these temperatures, pop-throughs may not be a meaningful concept. A plot of atomic positions in this higher T region is shown in Figure 4.

Harker-Patterson sections through the Patterson functions for several temperatures are very useful in understanding the structural disorder at the grain boundary. Figure 5 illustrates a projection of the Patterson function within $.1$ units of the $z = 0$ plane of the Ar system at $.055$ ($1/3$ the melting temperature), where z is the misorientation axis. Important features of this plot include its similarity to the dichromatic pattern, and the well-defined, spherical atomic positions, with blurring due to thermal excitation. Figure 6 is the same section of the system at a temperature of $.150$, but only the two planes on either side of each boundary were used to generate the Patterson function. The important feature of this plot is that though it is much more diffuse there is still a large amount of angular correlation. A liquid would be radially symmetric. However it should be pointed out that the interpretation of the high temperature Patterson functions is somewhat problematical. A thin layer of liquid sandwiched between two crystals would also be expected to exhibit in its Patterson function, some angular correlations characteristic of its adjacent crystals.

For all of the temperatures, we calculated thermodynamic averages of excess boundary properties using perfect crystal reference systems. The boundary excess enthalpies and volumes are plotted as a function of temperature in Figure 7. We see that until a temperature of $.12$ the excess properties are linear with T . In the temperature range of $.12$ to $.14$, we begin to see some deviations. We are still attempting to correlate these deviations with grain boundary structure variations. At $.135$, it is still possible to distinguish pop-throughs, whereas above $.140$ the region of the grain boundary is highly disordered, and the excess properties show marked increase. This, and the deviation of excess properties may be signs that a transition is occurring at about $.140$. The bulk melting temperature is about $.165$.

As temperature increases, the variation in thickness of the planes near the interface, as defined above, increases, though this effect is overwhelmed by the formation of pop-throughs. At all temperatures below $.140$ significant variations from a flat atomic plane occur only in the two planes nearest the interface, allowing for the observed pop-throughs.

SIMULATION OF NaCl $\Sigma 5$ TWIST BOUNDARIES

Our computational cell contains 12 layers of (002) planes with each plane containing 4 CSL unit cells. After the anti-coincidence ions are removed, the system has a total of 464 ions. The system contains two grain boundaries due to the application of periodic boundary conditions. The ions interact with the Born-Mayer-Huggins rigid ion potential parametrized by Fumi and Tosi for NaCl /15/. This potential has been extensively applied in constant volume molecular dynamics simulations of the bulk crystal and melt /16/ as well as crystal-vapor interfaces /17/ and thin crystalline films /18/ in alkali halides. The simulation of NaCl required major modifications of our flexible borders MD program in calculating the forces and potential because the existence of the electrostatic potential in ionic materials does not allow one simply to use a cut-off radius in calculating interacting forces. The traditional Ewald sum technique /19/ is applied to transform the Coulomb potential into two rapidly converging sums: one is in the real space and the other is in the reciprocal space. Both sums contain a parameter α which can be manipulated so that both sums converge rapidly with increasing r_{ij} and k , with r_{ij} the distance between particle i and j and k the distance between two reciprocal lattice points. It is a standard practice to spherically truncate both r_{ij} and k at values of r_c and k_{max} respectively. The choice of the parameter α and k_{max} is determined empirically by balancing accuracy and computing time requirements. A choice of $\alpha = 5.6/(2r_c)$, and a suitable value for k_{max} depending on the system size was found to be quite satisfactory for both the accuracy and rate of convergence. In this case, the real space part of the electrostatic potential, and force can be calculated together with short range potential and force with a cutoff radius r_c equal to 8.2\AA and the reciprocal space part of the force and potential is cut off at k^2 equal to 5\AA^{-2} . The real space calculation of force and potential has been made quite efficient by applying the Verlet list technique /20/ combined with the cell list technique /21/. Our calculations on melting and crystallization of a perfect NaCl system with 216 ions show that the thermodynamic properties of both crystal and melt are in good agreement with experimental results and previous constant volume MD simulations. Due to the application of periodic boundary conditions and the small system size the melting temperature estimated from this molecular dynamics simulation is ~ 1.7 in reduced units ($\sim 1220\text{K}$), which is about 150K higher than experimental results. The inclusion of ion polarizations, e.g. by a shell-model, is computationally prohibitive, and previous molecular dynamics simulations found that the rigid ion model to be quite adequate /22/.

Low Temperature Structure and Properties: We started with the anti-coincidence $\Sigma 5$ (001) twist boundary with one pair of anti-coincidence ions removed per CSL unit cell as in the molecular statics calculations by Tasker and Duffy /11/. We obtained the same boundary configurations as in their study of NiO upon taking out all the thermal energy of the system. The boundaries were heated up, at temperature intervals of $\sim 140\text{K}$, to the bulk melting temperature. Each run lasted 3000 or more time steps. This boundary configuration is very stable and planar (Fig. 8); it shows essentially no structural changes other than thermal expansion, up to $\sim 0.85T_m$, where T_m is the bulk melting point as determined by molecular dynamics simulations. We divided our system into 12 layers, delineated by minima in the density plot along the normal to the boundaries, and properties for each layer were calculated. The two layers adjacent to the boundary, along with the boundary layer, show higher potential energy (Fig. 9), which is easily understandable because of the low density of the boundary. We also calculated the stresses in the individual layers. The boundary is in a state of compression instead of tension, while the two neighboring layers to the boundary are in tension, as shown in Figure 10. Intuitively one would think that the boundary should be in tension due to its low density, but the point defects act as centers of dilation. The formation volume of a pair of Schottky defects in the bulk systems calculated by our molecular dynamics is 1.46Ω , where Ω is the molecular volume of NaCl, at zero temperature and increases with temperature. With so many defects in the boundary, the boundary tends to expand in the direction parallel to the boundary but is restricted by the adjacent layers. The structure factors for the boundary layers tend to decrease faster with increasing temperature than the layers away from the boundary (Fig. 11). The mean square displacements for the boundary layers were found to be larger than those of the bulk layers, which indicated greater thermal vibrations at the boundaries. From the analysis of the layer quantities, such as layer internal energy, two dimensional stresses and structure factors mentioned above, we find the boundary width to be extremely narrow: it essentially consists of only three (002) layers at low temperatures.

High Temperature Structure and Properties: The $\Sigma 5$ twist boundary in NaCl started to exhibit disorder at $\sim 0.85T_m$. This can be clearly seen in Figure 12, which is a projection of the average positions along the boundary. From a series analysis of atomic positions we found that the disordering process started with the motion of Schottky defects away from the boundary. The disordering is, therefore, not confined to the boundary plane but three planes at the early stage. In some of our simulations the boundary was observed to have migrated one plane within the time of simulation. This happened when most of the vacancies were replaced by the ions from one direction, either above or below the boundary. The increasing disorder is also indicated by the large

decrease in the structure factors from the boundary (Fig. 11). After the disorder started the boundary stresses relaxed to values close to zero as shown in Figure 10. The boundary width increases rapidly with increasing temperature once the boundary starts to become disordered. In fact at $\sim 0.90T_m$ the disordered region spreads to one half of the system during prolonged heating. The temperature is decreasing while the potential energy is increasing when the boundary is becoming disordered in this constant enthalpy molecular dynamics. The disordered structure, however, still maintains a degree of order as seen in the calculated structure factors (Fig. 11). The excess volume and excess enthalpy diverge as the temperature approaches the bulk melting temperature (Fig. 13). There is no indication of sudden changes in these excess quantities, which suggests that the grain boundary gradually becomes disordered as the melting temperature is approached and no definite temperature can be assigned as the grain boundary melting temperature.

DISCUSSION AND CONCLUSION

We performed molecular dynamics simulations of argon and NaCl $\Sigma 5$ (001) twist bicrystals and perfect crystal reference systems at temperatures ranging from low temperatures to the melting point. The simulations were performed under constant pressure in a molecular dynamics formulation which allows for volume and shape transformations of the computational simulation cell. We believe that this aspect is important in that it is unreasonable to study structural changes under a constant volume constraint.

The low temperature structure of the argon system features an expansion at the interface and relaxations of the coincident atoms. The planes at the interface are separated by ~ 1.2 times the interplanar spacing in a perfect crystal. The atoms at the coincident sites in the planes nearest the interface are displaced towards the interface by .104 units ($\sim 13\%$ of an interplanar spacing) with respect to the rest of the atoms in the that plane.

Only the CSL (no translation) state was found to be stable at low temperatures and constant pressure. We examined the Bristowe and Crocker Type 2 translation state under constant volume conditions and found that while it is metastable, the pressure on the sides of the simulation cell is anisotropic: twice as great perpendicular to the boundary plane as in the directions parallel to it. This points out the unphysical nature of constant volume grain boundary simulations.

In argon, at higher temperatures (from $1/3$ to $\sim .85 T_m$) a phenomenon which we call pop-throughs occur. These are regions where the four non-coincident site atoms in a plane adjacent to the boundary have fallen into the boundary and rotated into the orientation of the other crystal, thereby joining the other crystal and in effect moving the interface by one atomic layer. These pop-throughs involve an increase, though minor, in boundary enthalpy. As the temperature increases, they become increasingly common, and may occur in adjacent units. These may be postulated as a mechanism for grain boundary migration.

The $\Sigma 5$ (001) twist boundary in NaCl was found to be extremely stable in our dynamical simulations, which confirms the stability in Duffy and Tasker's calculation of molecular statics. No analogue to the pop-throughs observed in the argon boundaries occurred until at high temperatures at which the disordering process started.

Above $.85 T_m$, the twist boundary becomes disordered. The boundary consists of only three layers of (002) planes at low temperatures. It expanded rapidly upon disordering occurred. The disorder occurred by the motion of the Shottky vacancies away from the boundary and boundary migration can take place with all vacancies jumping in one direction.

Though the NaCl and Ar boundaries have different bonding type and very different low temperature structures, there are aspects of their high temperature which are similar. Disorder occurs in both systems although the relative temperature at which this begins is higher in NaCl than in Ar. The degree and the extent of disorder increase as the temperature is raised in both systems. The behavior of the excess enthalpy and volume are very similar in two systems which is continuous and increases rapidly once the disorder begins. The failure to locate any specific temperature lower than the bulk melting temperature at which the excess properties are discontinuous preclude us to assign a grain boundary melting temperature to both of the systems. Moreover, relative translations took place in both systems at high temperatures.

There are now a number of computer simulation studies that indicate that grain boundaries of various types and in various materials become highly disordered before bulk melting /23,24,25,26/. The detailed results of the simulations and the manner in which they have been interpreted, however, differ. In some studies, the excess thermodynamic properties of the grain boundary have been

observed to exhibit discontinuities at the onset of disorder and in others the changes have been more continuous. There have also been discrepancies in the degree and nature of disorder observed. These phenomena have been interpreted by various authors as grain boundary melting, grain boundary roughening, or as a continuous grain boundary disordering which does not involve a phase transition. Some of the discrepancies in behavior of model systems are due to differences in computational conditions, others to the use of different potential functions and yet other discrepancies may exist more in the interpretation than in the actual results. It seems plausible to assume that actual experimental systems may also exhibit a variety of behaviors depend on such factors as grain boundary type, the nature of interatomic bonding, and the segregation state. Experimentally, while there have been conflicting reports in the past, recent results indicate that at least some grain boundaries retain crystalline order virtually up to the melting point /27/. On the basis of the results reported here we conclude that although the $\Sigma 5$ twists in Ar and NaCl become highly disordered with temperature, remnants of crystalline spatial correlations are retained at the grain boundary up to the bulk melting point. Further calculations of the excess free energy throughout this temperature regime and the behavior of the boundary thicknesses with temperature would be useful to clarify the nature of this phenomenon.

ACKNOWLEDGEMENTS

This research was sponsored the Presidential Young Investigator Award of Gretchen Kalonji. We would like to express our gratitude to Dr. Manfred Rühle of the Institut für Werkstoffwissenschaften, Max-Planck Institut für Metallforschung, Stuttgart, for the hospitality and computational resources extended to us during the time spent by C. Counterman at his laboratory, where many of the computations were performed.

References

1. Deymier P. and Kalonji G., *J. de Physique* C4, 213 (1985).
2. Oh Y. and Vitek V., *Acta Metall.* 34, 1941 (1986).
3. Majid I. and Bristowe P., to appear in *Scripta Met.*
4. Carrion F., Kalonji G. and Yip S., *Scripta Met.* 17, 915 (1983).
5. Kalonji G., Deymier P., Najafabadi R. and Yip S., *Surf. Sci.* 144, 77 (1984).
6. Chaudhari P. and Matthews J. W., *J. Appl. Phys.* 42, 3063 (1971).
7. Sun C. P. and Balluffi R. W., *Phil. Mag.* A46, 49 (1982).
8. Wolf D., *Phil. Mag.* A49, 225 (1984).
9. Wolf D. and Benedek R., *Adv. in Ceram.* 1, 107 (1981).
10. Wolf D., *Adv. in Ceram.* 6, 36 (1983).
11. Duffy D. M. and Tasker P. W., *Phil. Mag.* A47, L45 (1983).
12. Parrinello M. and Rahman A., *J. Appl. Phys.* 52, 7182 (1982).
13. Warren B.E., "X-Ray Diffraction" (Addison Wesley, Reading, Mass.) 112.
14. Bristowe P. D. and Crocker A.G., *Phil. Mag.* A38, 487 (1978).
15. Tosi M. P. and Fumi F. G., *J. Phys. Chem. Solids* 25, 45 (1964).
16. Sangster M. J. L. and Dixon M., *Adv. in Phys.* 25, 247 (1976).
17. Heyes D. M., Barber M. and Clarke J. H. R., *J. Chem. Soc. Faraday Trans.* 2 75, 1469 (1979).
18. Heyes D. M., *J. Chem. Phys.* 79, 4010 (1983).
19. Ewald P. P., *Ann. Phys.* 21, 1087 (1921).
20. Verlet L., *Phys. Rev.* 159, 98 (1967).
21. Quentrec B. and Brot C., *J. Comp. Phys.* 1, 430 (1973).
22. Walker J. R., in "Computer Simulation of Solids", ed. by Catlow C. R. A. and Mackrodt W. C., P59 (1982).
23. Nguyen T., Ho P., Kwok T., Nitta C and Yip S., *Phys. Rev. Lett.* 57, 1919 (1986).
24. Broughton J. Q. and Gilmer G. H., *Phys. Rev. Lett.* 56, 2692 (1986).
25. Kikuchi R. and Cahn J.W., *Phys. Rev.* B21 1983 (1980).
26. Ciccotti G., Guillope M. and Pontikis V., *Phys. Rev.* B27, 5576 (1983).
27. Chan S.-W. and Balluffi R.W., *Acta. Met.* 33, 1113 (1985).

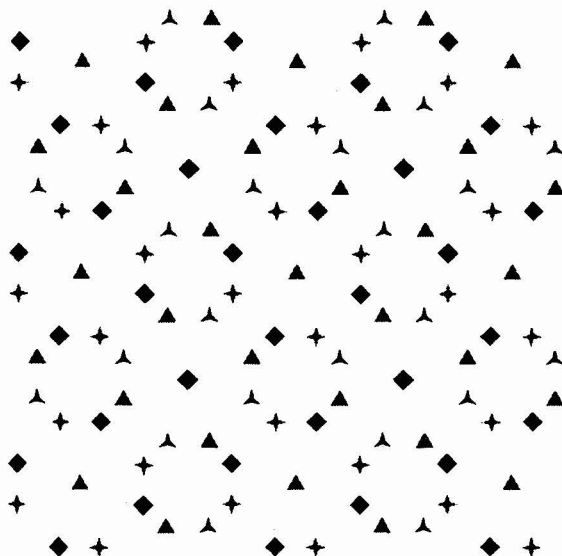


Figure 1. The relaxed $\Sigma 5$ twist boundary. The four planes nearest the boundary are shown. The twist axis is toward the viewer. The color of the polygons represents the elevation of the atom with respect to the average position of the atoms in the plane. The polygons with concave sides are in the planes nearest the interface except those at the coincident site. The number of points of the polygon shows the stacking sequence ABAB.

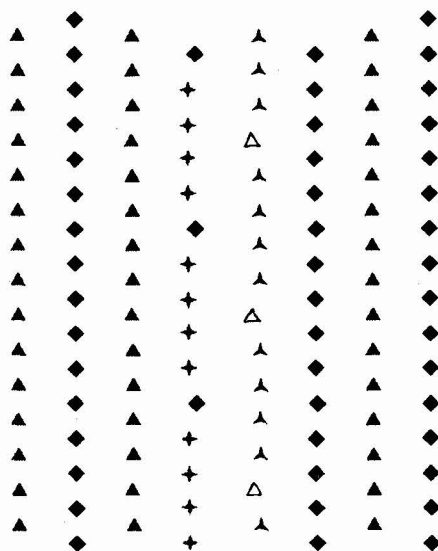


Figure 2. The relaxed $\Sigma 5$ twist boundary. The twist axis is toward the right. Eight planes nearest the boundary are shown. The colors and symbols are the same as in figure 1.

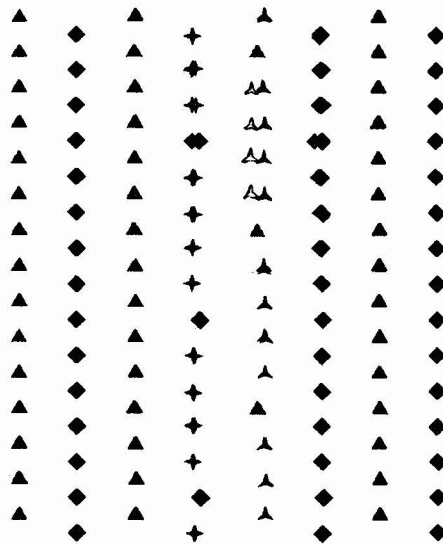


Figure 3. The $\Sigma 5$ twist boundary at $T = .055$. The twist axis is toward the right. The colors and symbols are the same as in Figure 1. The feature towards the top is a 'pop-through' the four atoms have moved down into the boundary, and rotated to the orientation of atoms in the other crystal.

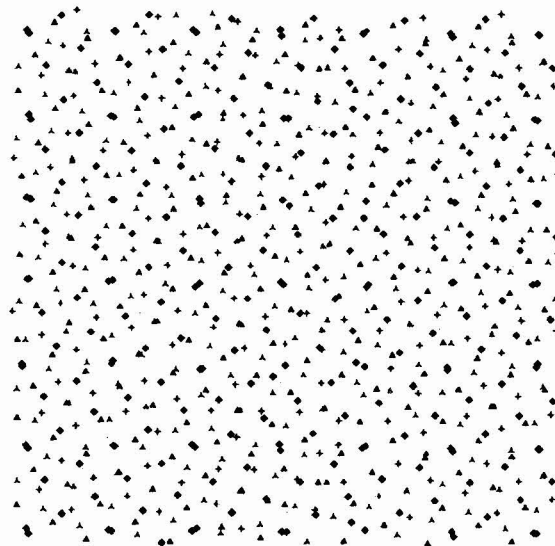


Figure 4. The $\Sigma 5$ twist boundary at $T = .150$. The twist axis is toward the right. The colors and symbols are the same as in Figure 1.

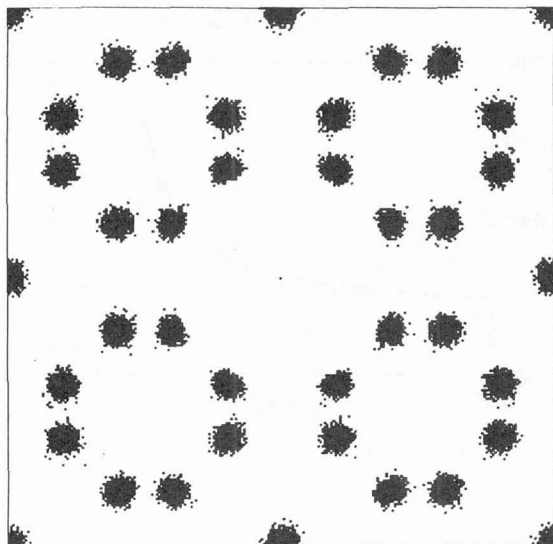


Figure 5. Section of the Patterson function of the $\Sigma 5$ twist argon bicrystal at $T = .055$, constructed from the instantaneous positions of the atoms. Shown is a section within .1 units of the $z=0$ plane of the Patterson function.

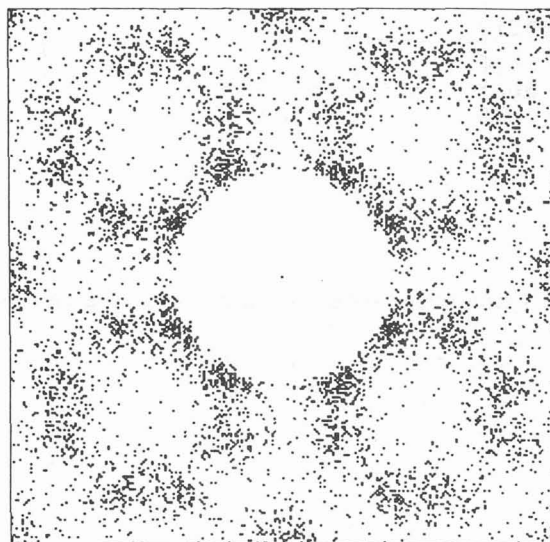


Figure 6. Section of the Patterson function of the $\Sigma 5$ twist argon bicrystal at $T = .150$, constructed from the instantaneous positions of the atoms. Shown is a section within .1 units of the $z=0$ plane of the Patterson function.

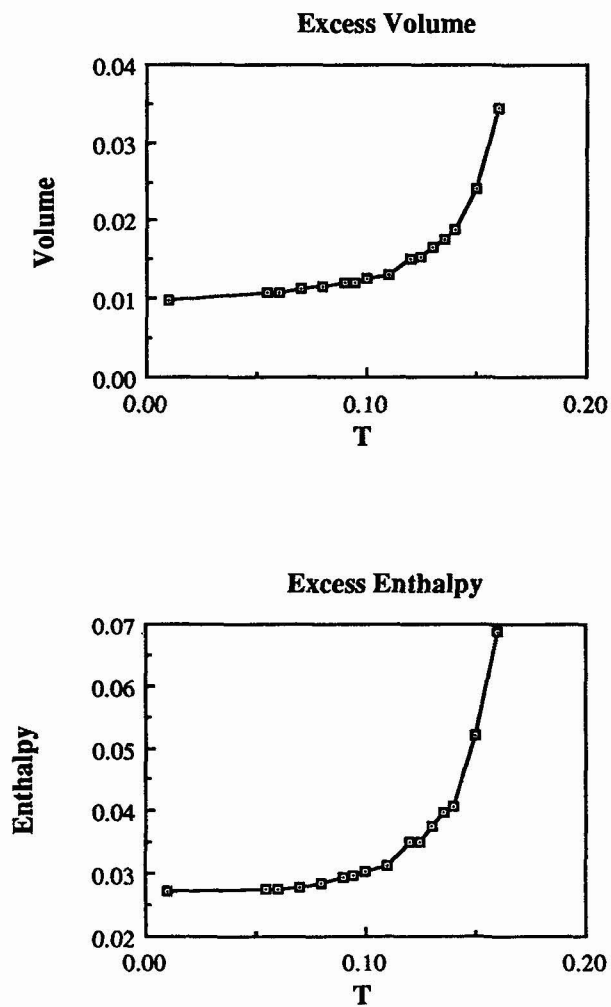


Figure 7. Excess volume and enthalpy as a function of temperature

Position plot

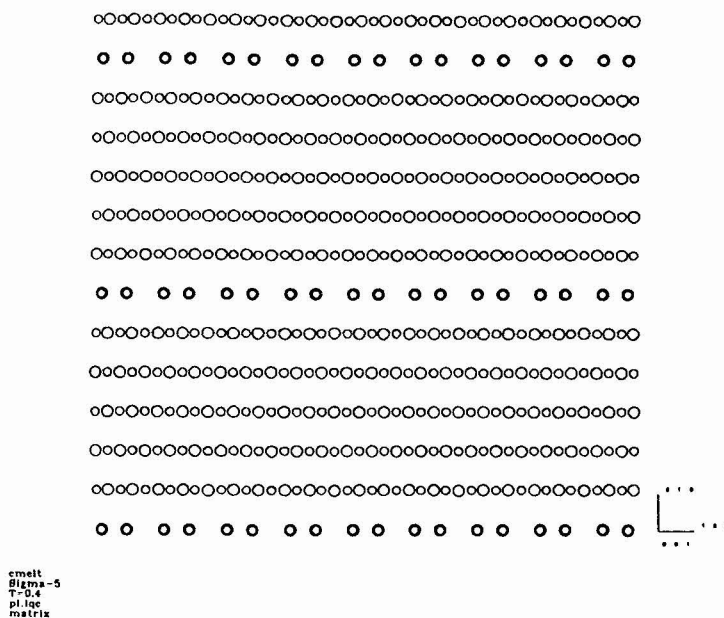


Figure 8. The projected structure of NaCl $\Sigma 5$ (001) twist boundary normal to the twist axis at temperature 0.4 ($\sim 290\text{K}$).

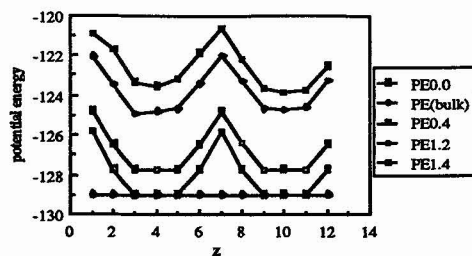


Figure 9. The layerwise potential energy per molecule along the twist axis at different temperatures.

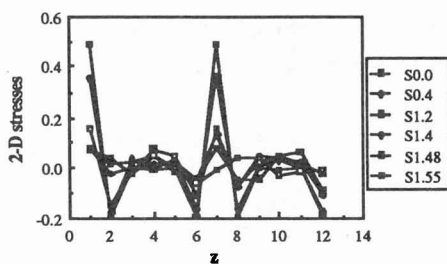


Figure 10. The two dimensional stresses $((\sigma_{xx} + \sigma_{yy})/2)$ parallel to the boundaries for each layer at different temperatures

